Appl. Phys. B (2014) 117:445–451
DOI 10.1007/s00340-014-5853-7

Applied Physics B
Lasers and Optics

QCL-based TDLAS sensor for detection of NO toward emission measurements from ovarian cancer cells

M. Köhring · S. Huang · M. Jahjah · W. Jiang · W. Ren · U. Willer · C. Caneba · L. Yang · D. Nagrath · W. Schade · F. K. Tittel

Received: 12 March 2014 / Accepted: 20 April 2014 / Published online: 8 May 2014

Abstract The development of a sensitive sensor for detecting nitric oxide (NO) emissions from biological samples is reported. The sensor is based on tunable diode laser absorption spectroscopy (TDLAS) using a continuous wave, thermoelectrically cooled quantum cascade laser (QCL) and a 100-m astigmatic Herriot cell. A 2*f*-wavelength modulation spectroscopy technique was used to obtain QCL-based TDLAS NO emission measurements with an optimum signal-to-noise ratio. An absorption line at 1,900.076 cm^{-1} was targeted to measure NO with a minimum detection limit of 124 ppt. Positive control measurements with the NO donor DETA NONOate were performed to determine and optimize the sensor performance for measurements of biological samples. Our measurements with NO donor show the potential suitability of the sensor for monitoring NO emission from cancer cells for biological investigations.

M. Köhring · S. Huang · M. Jahjah · W. Jiang · W. Ren · C. Caneba · L. Yang · D. Nagrath · F. K. Tittel (✉)
Rice University, 6100 Main St., Houston, TX 77005, USA
e-mail: fkt@rice.edu

M. Köhring (✉) · W. Schade
Fraunhofer Heinrich-Hertz-Institute, Am Stollen 19B, 38640 Goslar, Germany
e-mail: michael.koehring@hhi.fraunhofer.de

S. Huang
Princeton University, Princeton, NJ 08540, USA

U. Willer
EFZN, Clausthal University of Technology, Am Stollen 19B, 38640 Goslar, Germany

1 Introduction

Nitric oxide (NO) is a small molecule forming an odorless, colorless, and highly reactive gas. The role of this radical in various interaction processes with biological tissue is significant [1, 2], even leading to a Nobel Prize for physiology and medicine in 1998 [3]. Especially in the field of carcinogenesis and tumor growth suppression, NO plays an important role. It can be produced by cancer cells in low concentrations, and at these concentrations, NO can increase proliferation. On the other hand, high concentrations of NO can suppress tumor growth [4–7].

Ovarian cancer is the leading cause of gynecological cancer-related deaths, and ~14,270 US women will die of ovarian cancer in 2014 [8]. Ovarian cancer is usually detected at late stages, when metastasis has already occurred to distant sites, such as at the lining of the abdomen and lymph nodes [9–11]. The expression level of induced nitric oxide synthetase (NOS), an enzyme responsible for converting arginine into citrulline and thereby producing nitric oxide, is higher in poorly differentiated tumors compared to benign tissues. These findings indicate a potential correlation between tumor malignancy and NOS enzymatic activity [12]. However, a comprehensive understanding for processes linking the effects of NO on ovarian cancer cells tumorigenicity and malignancy is unknown. Therefore, detailed temporal and quantitative information of the NO emission from cancer cells can lead to a more precise insight into phenomena associated with basic biological studies. Currently used techniques for measuring NO emissions are not capable of providing cross sensitivity and interference free, quantitative, and time resolved information. Therefore, an entirely optical approach was developed to provide information about NO concentrations and associated temporal emission dynamics.

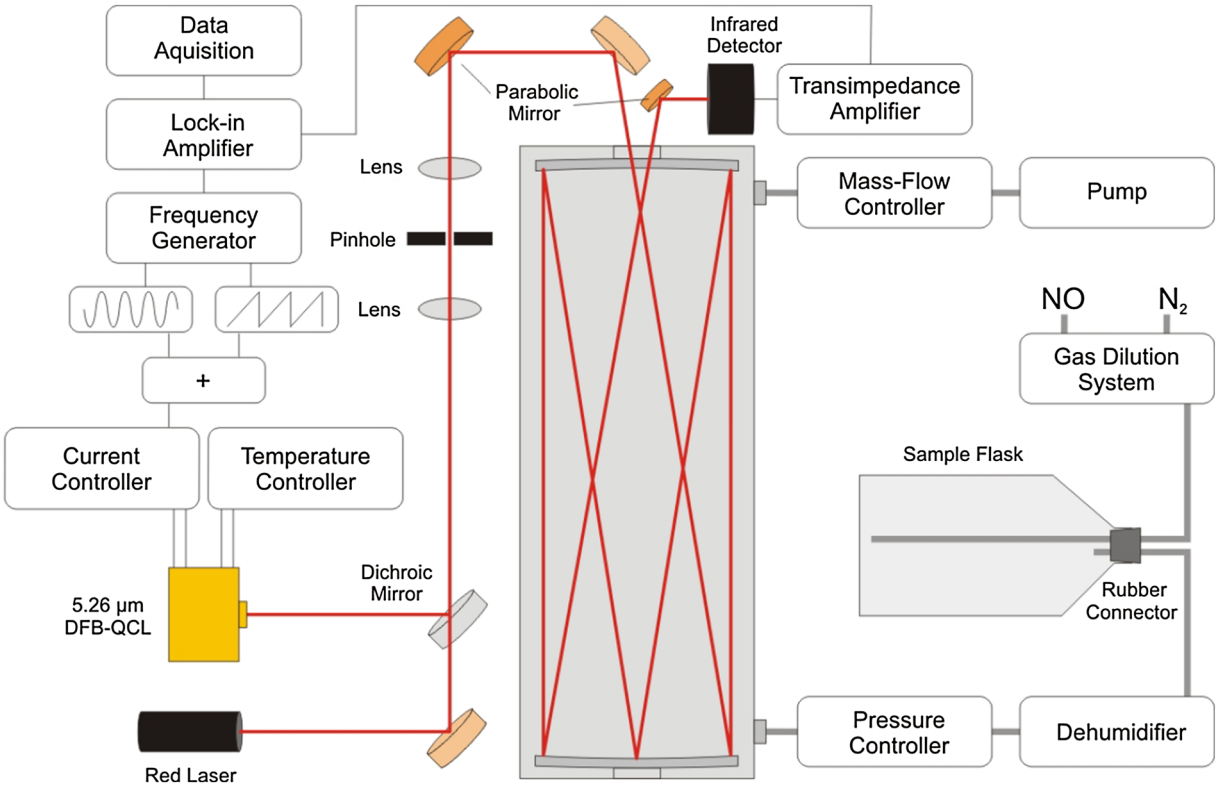

Fig. 1 Schematic of NO sensor system, including optical, electrical, and gas flow pathways

The realization of the quantum cascade laser (QCL) by Faist et al. [13] and its further development in the following years [14] has enabled great progress in several fields of optical technology including medical diagnostics [15–17]. The commercial availability of mid-infrared, tunable, narrow-line-width semiconductor lasers with considerable optical output power addressing the fundamental absorption lines of many molecules enables the use of laser spectroscopy for sensitive and selective detection in numerous applications including medical diagnostics. In particular, the availability of thermoelectrically cooled (TEC), continuous wave (CW), distributed feedback (DFB) QCLs with optical output powers in the mW range allows the development of highly accurate and compact optical sensors with minimum detection limits in the ppb or even ppt range [18–21].

In this article, we report a NO sensor, which consists of a 5.26-µm CW DFB QCL and an astigmatic Herriot multipass cell. Such a sensor permits sensitive and selective NO emission detection based on a 2*f*-wavelength modulation tunable diode laser absorption spectroscopy (TDLAS) technique. Measurements were performed with certified NO in N_2 gas mixtures and NO donor samples. Such a sensor platform permits measurement of NO from ovarian cancer cells.

2 Experimental setup

A schematic of the NO sensor platform is shown in Fig. 1. A TEC CW QCL [from Alpes Lasers (lower left in Fig. 1)] emits ~4 mW of optical power at a wavelength of 5.26 µm using a current controller (ILX Light wave LDX-3220) and thermally stabilized with a temperature controller (Wavelength Electronics MPT-5000). For optical alignment purposes, a red diode laser beam was superimposed on the mid-infrared (MIR) QCL beam by means of a dichroic beam splitter. A pair of lenses placed in combination with a pinhole (400 µm in diameter) was used for spatial filtering to optimize the shape of the MIR beam, which reduced the optical power to ~2 mW. After the second lens, two mirrors were used to direct the QCL beam into the multipass cell. After 182 passes in the astigmatic Herriot cell (Aerodyne Inc.), a parabolic mirror was used to send the QCL beam to the cryogenically cooled MIR detector (Kolmar Technology KMPV10-1-J1/D0), which was equipped with an additional thermal insulation to enhance the NO sensor stability.

Measurements showed that a stable pressure is required as even slight changes in the system pressure resulted in sensor baseline shift. Therefore, both system pressure and gas flow were regulated by a pressure controller and a mass flow controller, respectively. A 2-stage oil free diaphragm

pump was used to maintain a measurement pressure of 300 Torr. To provide different NO concentration levels for calibration measurements, a gas dilution system (Environics, Inc.) was used to dilute a certified 1.2-ppm NO mixture with purified nitrogen. The chamber for the biological samples was positioned in between the gas dilution system and the pressure controller. This ensures that the biological samples are kept continuously at ambient pressure to conserve favorable conditions for the cancer cells. Temperature stabilization was applied to the base of the cell chamber to maintain the sample temperature at a constant 37 °C throughout the measurements. A dehumidifier was used to avoid the formation of water droplets on the multipass cell mirrors and windows.

A 2*f*-wavelength modulation technique [22, 23] and a lock-in amplifier were used to increase the TDLAS-based signal-to-noise ratio (SNR). A fast (10 kHz) sinusoidal wave and a slow (1 Hz) saw tooth wave provided by a function generator (Tektronix AFG3022B) were superimposed on the QCL driver current to modulate the laser and to sweep across the targeted NO absorption feature. The second harmonic of the signal from the MIR detector was acquired by a trans-impedance amplifier followed by a lock-in amplifier (Signal Recovery 7265 DSP). Data acquisition (DAQ) was implemented with a DAQ card (NI-DAQ-AI-16XE-50) and a laptop using National Instruments LabView software.

3 NO sensor calibration

The QCL was chosen to target an optimum absorption line at 5.26 μm, corresponding to a wavenumber of 1,900.076 cm^{-1} with a width of $\sim 0.049 \pm 0.001$ cm^{-1}. Four different NO concentration levels balanced with pure N_2 were measured. Each concentration level was held for ~ 30 min using the gas dilution system described in Sect. 2. Figure 2 shows the normalized sensor signal versus NO concentration. The error bars at each data point indicate the standard deviation (1σ) of the NO sensor signal for steady state conditions. The inset depicts the temporal behavior during NO emission measurements, starting with pure N_2, followed by four NO concentration levels starting from the lowest level, and ending with a final period of pure N_2. For the two lowest concentration levels, equilibrium is only achieved after a peak value at the beginning of each concentration step. This is due to the gas dilution system operated at a high dilution rate but which has no influence on the NO sensor performance for biological samples. The baseline-corrected spectra corresponding to the four concentrations obtained at the end of each 30-min period are shown in Fig. 3. As expected for small concentrations, the sensor signal (Fig. 2) shows a nearly linear dependence of the NO concentration. An exponential fit function was numerically applied to the data points in Fig. 2, which indicated a good agreement with Beer–Lambert law. The NO sensor minimum detection limit (MDL) was estimated to be 0.512 ± 0.05 ppb by calculating the first derivative of the exponential fit at zero NO concentration. The SNR can be further optimized by means of signal averaging [24]. Hence, an Allan deviation was performed by measuring the NO mixture with a constant concentration of 120 ppb as shown in Fig. 4. The MDL obtained by signal averaging is achieved with an averaging time of 160 s for the NO sensor. Furthermore, the MDL can be decreased to 124 ppt using the significantly smaller noise level of the sensor signal corresponding to the optimum averaging time.

4 Positive control measurements

The use of NO donor molecules is a state-of-the-art approach to create a NO signal similar to NO emission from biological samples [7, 25, 26] and to enable positive control measurements for the NO sensor. Such donor molecules emit NO following an exponential decay which increases at higher temperatures. In this work, the NO donor molecule DETA NONOate ($C_4H_{13}N_5O_2$) was used. The half life of the donor molecule is ~ 20 h at 37 °C, and 2 mol of NO per mole of donor are delivered. To replicate the NO emission of cancer cells, the donor molecules were dissolved in the growth medium RPMI, which was also used for the ovarian cancer cell sample describe in Sect. 5. All samples were prepared in growth flasks with a flat base of area 175 cm^2 on which a liquid layer of ~ 2 mm thickness consisting of the growth medium and donor molecules or the cancer cells is located. The flask size was chosen to be of this size as the surface area of the growth medium liquid determines the number of cancer cells which can exist per sample. As each molecule emits a certain amount of NO, a higher number of cells will increase the number of NO molecules in the sample chamber. The polymer flasks were attached to the sensor gas flow system by inserting a rubber connecting section into the flask neck, containing two metal tubes with different lengths, to ensure good mixing of the pure N_2 and the gas emitted from the biological samples (see Fig. 1).

NO donor emission spectra were collected over a time period of ~ 60 min to investigate the temporal signal behavior of the NO sensor. Each line in Fig. 5 represents the average of over 100 spectra taken from the sensor, starting with the solid black line ~ 3 min after insertion of the donor and ending with the dotted black curve after 60 min. The rise time of the signal corresponds to the low

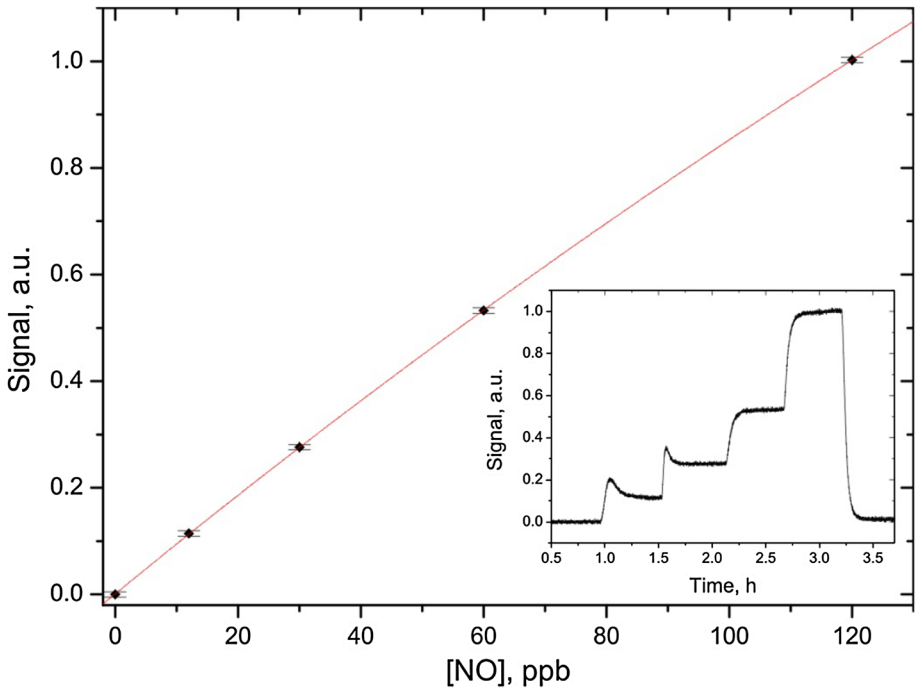

Fig. 2 Plot of the sensor signal behavior for different NO concentration levels (*black squares*) and an exponential fit to these data points (*red line*); inset shows the corresponding temporal behavior

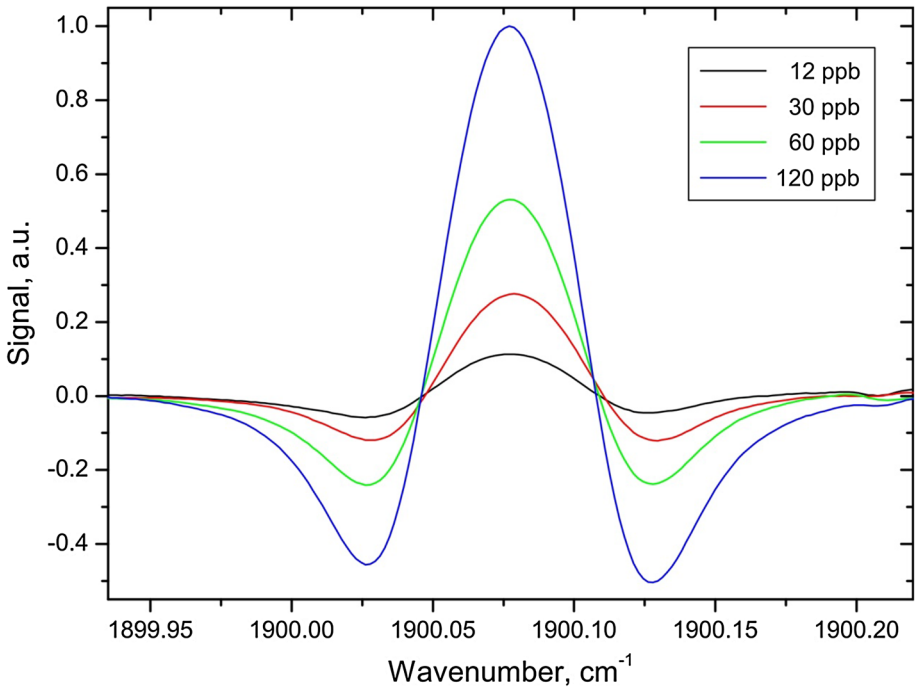

Fig. 3 NO spectra obtained at four ppb concentration levels (12, 30, 60, and 120 ppb) depicting both the characteristic 2*f* line shape and the NO concentration dependence

flow rate used for this experiment. For a flow rate of 50 sccm, the gas exchange of the whole measurement system takes ~60 min for the multipass gas cell volume (3 l). This value corresponds to the temporal dependence of the donor signal as seen in the inset of Fig. 5.

The reason for using such a small flow lies in the emission characteristics of biological samples. The NO concentration in the gas mixture leaving the sample chamber should increase with a decreasing N_2 flow as the number of NO molecules emitted from cancer cell and donor samples does not depend on the N_2 flow through the sample chamber. To verify this hypothesis, measurements with different N_2 flow rates were carried out without changing other measurement parameters, and the results are shown in Fig. 6. Each data point represents the maximum NO signal measured for the donor at a flow rate of

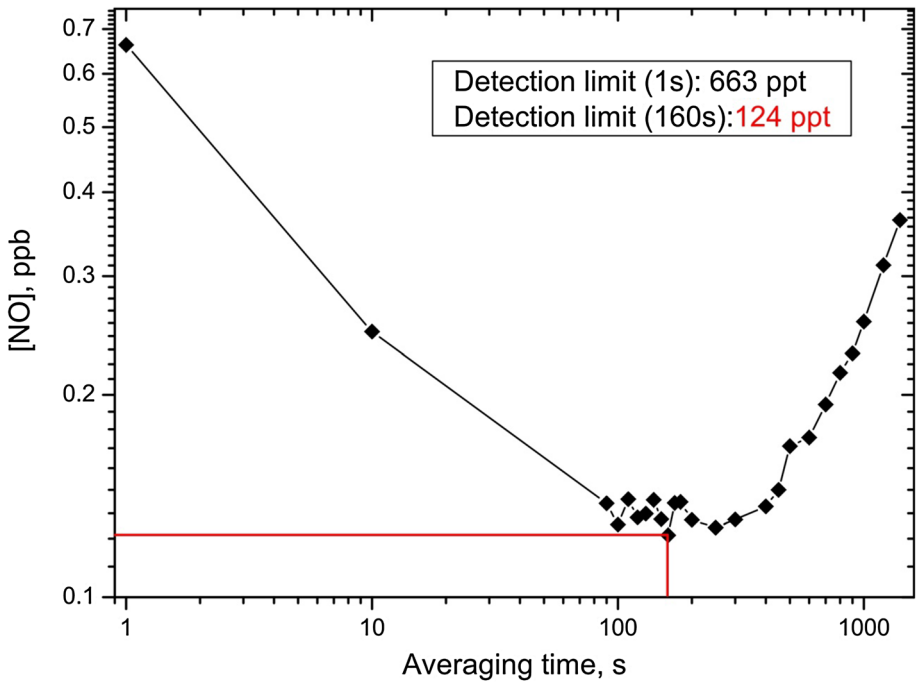

Fig. 4 Allan deviation was derived for several averaging times, and the optimum averaging time for the sensor system was determined to be 160 s

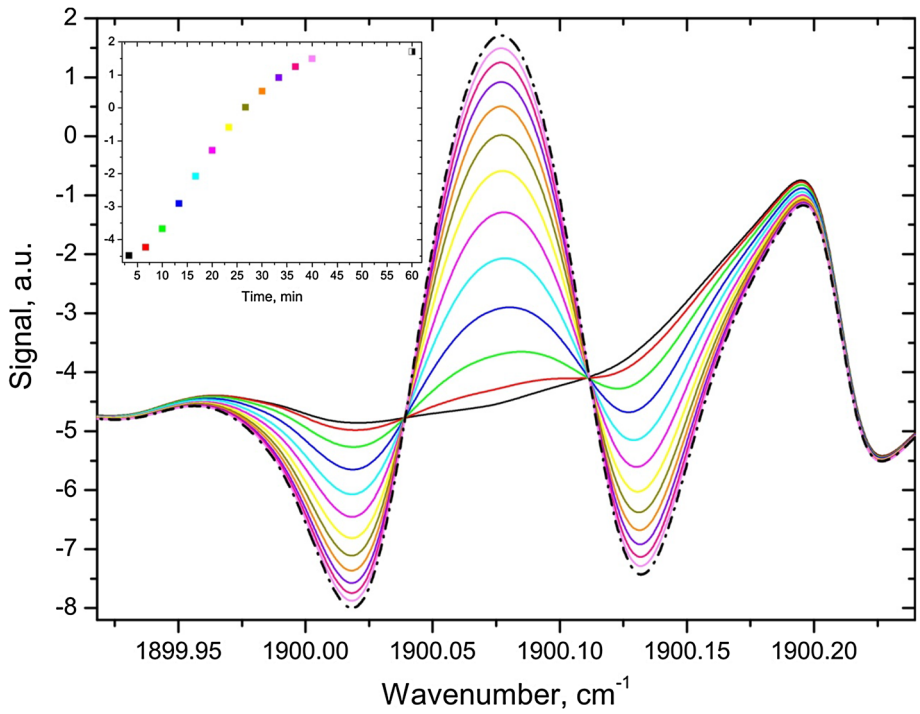

Fig. 5 Temporal dependence of the sensor signal, measured with the NO donor used for positive control measurements. *Inset* shows the temporal development of the peak value of the NO absorption line

800, 400, 200, or 100 sccm. An exponential fit was applied to the data to extrapolate the signal behavior for even lower nitrogen flows. The inset of Fig. 6 shows the average of 100 spectra for each flow, taken at equilibrium conditions. Based on the results from these measurements, the N_2 flow for the cancer cell measurements was chosen to be 50 sccm. A decrease in the system N_2 flow from 800 to 50 sccm leads to a significantly stronger signal strength by a factor of $\sim$20. The time needed to achieve stable measurement conditions is determined by the gas exchange time, e.g., for 50 sccm, it takes $\sim$60 min (see Fig. 5). While comparatively slow for an optical technique, this assures that the percentage of living cells in a biological sample is high.

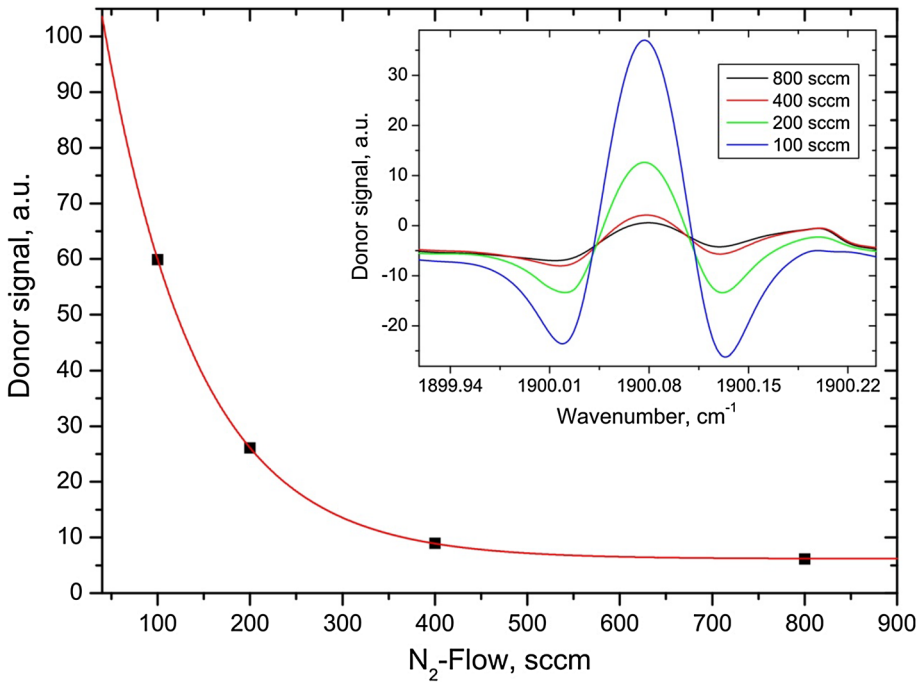

Fig. 6 Dependence of the NO donor signal from biological samples as a function of the gas flow rate (*black squares*). An exponential fit (*red line*) was applied to the data points to show the signal behavior for lower flow rates. *Inset* shows measured spectra corresponding to the flow rates

5 Conclusions

The development of a TDLAS sensor for NO detection of cancer cell emissions is reported. A CW TEC DFB QCL at a wavelength of $\sim$5.26 μm was used in combination with 2*f*-wavelength modulation spectroscopy and a 100-m absorption path astigmatic Herriot cell. Calibration measurements show a MDL of 0.512 ± 0.05 ppb without averaging. From an Allan deviation plot, an optimum averaging time of 160 s was determined, which corresponds to a MDL of $\sim$124 ppt.

Positive control measurements with a NO donor were performed to optimize the sensor performance for biological samples. According to these measurements, the total flow rate through the sample chamber was chosen to be 50 sccm. First measurements with ovarian cancer cells demonstrated the capability of the reported QCL-based TDLAS sensor for measuring the NO emission of cancer cells. Future experiments with different types of cancer cells and various treatment methods will follow to investigate the behavior of the NO emission and to explore the metabolism of various cell types in further detail as well as the use of cavity ring down spectroscopy instead of TDLAS, and a commercial Sievers NO analyzer based on ozone chemiluminescence [27].

Acknowledgments The authors acknowledge Dr. C. Bauer from Testo AG, Germany, for providing the CW TEC DFB QCL.

References

1. D. Fukumura, S. Kashiwagi, R.K. Jain, Nat. Rev. Cancer **6**, 521 (2006)
2. W. Xu, L.Z. Liu, M. Loizidou, M. Ahmed, I.G. Charles, Cell Res. **12**, 311 (2002)
3. R. SoRelle, Circulation **98**, 2365 (1998)
4. L. Thomsen, D. Miles, Cancer Metastasis Rev. **17**, 107–118 (1998)
5. A.J. Hobbs, A. Higgs, S. Moncada, Annu. Rev. Pharmacol. Toxicol. **39**, 191 (1999)
6. S. Mocellin, V. Bronte, D. Nitti, Med. Res. Rev. **27**, 317 (2007)
7. S. Huerta, S. Chilka, B. Bona Vida, Int. J. Oncol. **33**, 909 (1992)
8. American Cancer Society, Cancer facts and figures 2014 (American Cancer Society, Atlanta), www.cancer.org
9. C.A. Caneba, N. Bellance, L. Yang, L. Pabst, D. Nagrath, Am. J. Physiol. Endocrinol. Metab. **303**, E1036 (2012)
10. S.A. Cannistra, N. Engl. J. Med. **351**, 2519–2529 (2004)
11. R.C. Bast Jr., B. Hennessy, G.B. Mills, Nat. Rev. Cancer **9**, 415–428 (2009)
12. L.L. Thomsen, F.G. Lawton, R.G. Knowles, J.E. Beesley, V. Riveros-Moreno, S. Moncada, Cancer Res. **54**, 1352–1354 (1994)
13. J. Faist, F. Capasso, D.L. Sivco, C. Sirtori, A.L. Hutchinson, A.Y. Cho, Science **264**, 553 (1994)
14. C. Gmachl, F. Capasso, D.L. Sivco, A.Y. Cho, Rep. Prog. Phys. **64**, 1533 (2001)
15. Robert.F. Curl, F. Capasso, C. Gmachl, A.A. Kosterev, B. McManus, R. Lewicki, M. Pusharsky, G. Wysocki, F.K. Tittel, Chem. Phys. Lett. **487**, 1 (2010)
16. A. Kosterev, G. Wysocki, Y. Bakhirkin, S. So, R. Lewicki, M. Fraser, F. Tittel, R. Curl, Appl. Phys. B **90**, 165 (2008)
17. S. Barbieri, J.-P. Pellaux, E. Studemann, D. Rosset, Rev. Sci. Instrum. **73**, 2458 (2002)
18. D.D. Nelson, J.H. Shorter, J.B. McManus, M.S. Zahniser, Appl. Phys B. **75**, 343–350 (2002)

19. J.B. McManus, J.H. Shorter, D.D. Nelson, M.S. Zahniser, D.E. Glenn, R.M. McGovern, Appl. Phys. B **92**, 387 (2008)
20. J.B. McManus, M.S. Zahniser, D.D. Nelson, Appl. Opt. **50**, A74 (2011)
21. R. Lewicki, G. Wysocki, A.A. Kosterev, F.K. Tittel, Opt. Express **15**, 7357 (2007)
22. S. Schilt, L. Thévenaz, P. Robert, Appl. Opt. **42**, 6728 (2003)
23. S. Schilt, L. Thévenaz, Infrared Phys. Technol. **48**, 154 (2006)
24. P. Werle, R. Mücke, F. Slemr, Appl. Phys. B. **57**, 131 (1993)
25. J.A. Hrabie, J.R. Klose, D.A. Wink, L.K. Keefer, J. Org. Chem. **58**, 1472 (1993)
26. L.K. Keefer, R.W. Nims, K.M. Davies, D.A. Wink, "NONOates" as nitric oxide donors: convenient nitric oxide dosage forms, in *Nitric Oxide Part A: Sources and Detection of NO; NO Synthase*, ed. by L. Packer (Academic Press, New York, 1996)
27. GE Water & Process Technologies, Analytical Instruments, Boulder, CO, www.geinstruments.com